

GA-A23392

**INITIAL IMPLEMENTATION OF A MULTIVARIABLE  
PLASMA SHAPE AND POSITION CONTROLLER  
ON THE DIII-D TOKAMAK**

by  
D.A. HUMPHREYS, M.L. WALKER, J.A. LEUER, J.R. FERRON

JUNE 2000

## DISCLAIMER

This report was prepared as an account of work sponsored by an agency of the United States Government. Neither the United States Government nor any agency thereof, nor any of their employees, makes any warranty, express or implied, or assumes any legal liability or responsibility for the accuracy, completeness, or usefulness of any information, apparatus, product, or process disclosed, or represents that its use would not infringe privately owned rights. Reference herein to any specific commercial product, process, or service by trade name, trademark, manufacturer, or otherwise, does not necessarily constitute or imply its endorsement, recommendation, or favoring by the United States Government or any agency thereof. The views and opinions of authors expressed herein do not necessarily state or reflect those of the United States Government or any agency thereof.

# **INITIAL IMPLEMENTATION OF A MULTIVARIABLE PLASMA SHAPE AND POSITION CONTROLLER ON THE DIII-D TOKAMAK**

by

**D.A. HUMPHREYS, M.L. WALKER, J.A. LEUER, J.R. FERRON**

This is a preprint of a paper to be presented at the IEEE International Conference on Controlled Applications and IEEE International Symposium on Computer-Aided Control System Design, September 25-27, 2000, Anchorage, Alaska to be published in the Proceedings.

Work supported by  
the U.S. Department of Energy  
under Contract No. DE-AC03-99ER54463

**GA PROJECT 30033  
JUNE 2000**

**ABSTRACT**

A model-based multivariable controller for plasma shape control has been successfully implemented on the DIII-D tokamak. Good steady-state control of the plasma boundary shape and X-point position was demonstrated in lower single-null ohmic plasmas over several seconds of several discharges. Dynamic control for programmed rapid plasma shape variation showed significant lags in response (resulting from design choices and model error, and expected from simulation), but was robustly stable for all degrees of freedom explored. The control design was based on a linear plasma response model derived from fundamental physics assumptions, which was extensively validated against DIII-D experimental data. This physics-based model is readily extendable to next-generation device designs and to new operating regimes of existing devices. Controllers produced with robust control design methods were tested and improved using results of closed loop simulations. A comprehensive simulation of the tokamak plant including plasma response, power supplies, and coil circuit configuration allowed verification of the controller implementation in the plasma control system. This comprehensive simulation can be regulated by the plasma control system computer in exactly the same way the plasma control system controls the actual tokamak.

**1. INTRODUCTION**

Plasma equilibrium control in tokamaks is a fundamentally multivariable task, typically actuating 10–20 control coils to regulate 5–15 parameters describing the plasma position and shape. Currents driven in the control coils produce magnetic fields which interact with the current carried by the plasma, changing the plasma shape or position. Plasma control systems typically must maintain the overall plasma position and shape with accuracies better than 0.5% of the plasma width and stabilize plasmas against intrinsically unstable vertical displacements. The need for significant accuracy in the presence of an instability with growth times comparable to the time required for the actuating magnetic fields to reach the plasma poses a significant challenge to a plasma control system (PCS). Despite this, relatively little use has been made of modern multivariable control design methods in operating tokamak experiments to date. The most extensive and successful implementation of model-based multivariable controllers on a tokamak was

achieved by a collaboration between the TCV device team and the CREATE consortium [1,2].

The present work describes the successful initial implementation and experimental test of a model-based multiple-input-multiple-output (MIMO) algorithm for control of plasma shape and position on the DIII-D tokamak. In contrast with [1], this controller was based on a “minimal” plasma response model [3] and regulated a large number of shape and position quantities (~15), comparable to the number of independent control coil circuits (~17). This implementation made use of the “isoflux” shape control scheme used routinely in DIII-D which allows highly detailed control of the plasma boundary and position [4]. However, while the baseline control algorithm includes proportional, integral, and derivative (PID) matrix gain capability, the (largely diagonal) gain matrix is presently determined through empirical means, and system performance is typically improved during machine operations using between-shot experience. Development of a system for design of robust multivariable controllers based on validated models of plasma, conductor, and power supply responses is expected to improve the overall control quality and reduce the time required to obtain a satisfactory control algorithm.

Section 2 summarizes the present shape control system in routine use at DIII-D. Section 3 describes the system response model used in design of the controllers. The controller design approach itself is discussed in Section 4, along with simulation tools used for validation of the system model and assessment of controller performance. A summary and conclusions are presented in Section 5.

**2. DIII-D PLASMA SHAPE CONTROL**

In recent years, the control methodology at DIII-D has changed from its original combination of gap and “flux ratio” control [5] to “isoflux” control [4]. The isoflux control method, now in routine use on DIII-D, exploits the capability of the new realtime EFIT plasma equilibrium reconstruction algorithm to calculate total magnetic flux at specified locations within the tokamak vacuum vessel. Figure 1 illustrates a lower single-null (LSN) plasma which was controlled using isoflux control and indicates quantities relevant to the control scheme. The realtime EFIT algorithm can calculate the value of flux in the vicinity of the plasma boundary very accurately. Thus, the controlled parameters are the values of flux at prespecified control points

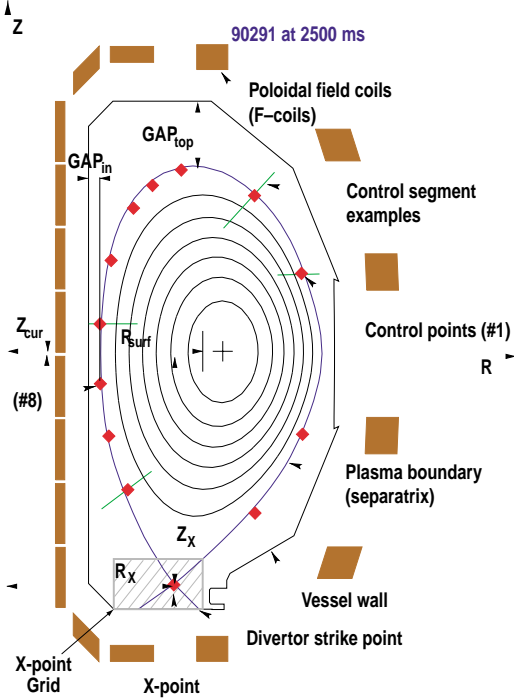


Fig. 1. Example of controlled plasma parameters in isoflux control scheme:  $R_X$ ,  $Z_X$ , and flux at 13 control points specified to be on the plasma boundary.

along with the X–point radial position ( $R_X$ ) and vertical position ( $Z_X$ ). By requiring that the flux at each control point be equal to the same constant value, the control forces the same flux contour to pass through all of these control points. By choosing this constant value equal to the flux at the X–point, this flux contour must be the last closed flux surface or separatrix. The desired separatrix location is specified by selecting one of a large number of control points along each of several control segments. An X–point control grid is used to assist in calculating the X–point location by providing detailed flux and field information at a number of closely spaced points in the vicinity of the X–point.

Present DIII–D operations use the isoflux control method with PID operations on the control point flux and X–point  $R_X$  and  $Z_X$  errors. The resulting PID signals are multiplied by a gain matrix to produce commands to the pulse width-modulated (chopper) power supplies on each plasma shaping coil. The gain matrix is sparse, so that most individual shape errors are corrected through the application of only a small number (often one) of coil voltage changes. Control of the X–point requires coordinated action by the largest number (4) of shaping coils.

### 3. MODEL-BASED MULTIVARIABLE CONTROLLER DESIGN AND SIMULATION

The new model-based multivariable controller developed for this initial implementation produces fully coupled

multivariable control. The controller design is derived from a linear model of the system to be controlled (plasma, conductors, power supplies) and incorporates knowledge of the time response of all outputs (flux and X–point errors) due to each input (chopper voltages). A linearized plant model was developed and extensively validated [6,3] in order to enable the use of mature linear multivariable design techniques.

#### 3.1. System Model and Controller Design

The system of plasma, shaping coils, and passive structure can be described using circuit equations derived from Faraday’s Law (e.g., [7,8]). These circuit equations take the following form when the effects of plasma motion as well as variation in plasma current are made explicit:

$$M_{ss} \frac{dI_s}{dt} + R_{ss} I_s + M_{sp} \frac{dI_p}{dt} + I_{p0} \frac{\partial M_{sp}}{\partial z_c} \frac{dz_c}{dt} + I_{p0} \frac{\partial M_{sp}}{\partial R_m} \frac{dR_m}{dt} = V_s \quad (3-1)$$

where the subscript “s” refers to all stabilizing conductors,  $I_s$  is the vector of (perturbed) conductor currents,  $I_p$  is the (perturbed) plasma current,  $z_c$  is the vertical position of the plasma current centroid, and  $R_m$  is the major radial position of the magnetic axis.

Radial and vertical force balance relations, assumption of rigid radial and vertical displacement of the equilibrium current distribution, and specification of a resistive plasma circuit equation closes this set of system equations. The circuit equation then becomes

$$\begin{aligned} & (M_{ss} + X_{ss}) \frac{dI_s}{dt} + R_{ss} I_s + \\ & (M_{sp} + X_{sp}) \frac{dI_p}{dt} + \\ & X_{s\beta} \frac{d\beta_p}{dt} + X_{sI} \frac{dI_i}{dt} = V_s \quad (3-2) \end{aligned}$$

where  $X_{ss}$  represents the variation of conductor flux due to plasma motion in response to conductor current variation,  $X_{sp}$  represents variation in conductor flux due to plasma motion in response to plasma current variation,  $M_{sp}$  is the mutual coupling from plasma to conductors, and  $X_{s\beta}$  and  $X_{sI}$  describe the variation in conductor flux due to plasma motion in response to variations in  $\beta_p$  and  $I_i$ . The circuit connections in DIII–D cause the individual objects to be modified somewhat from their initial values calculated from independent coil currents, but the form of the equations remains the same. In Eq. (3–2) the state of the system is entirely described by the conductor and plasma currents ( $I_s$ ,  $I_p$ ), while perturbations of  $\beta_p$  and  $I_i$  from their equilibrium values are treated as exogenous variables.

The plasma current dynamic response is governed by a circuit equation similarly derived from Faraday’s Law

which treats the plasma as a single circuit consisting of a distributed array of conducting elements. The self-inductance  $L_p$  is derived from this equilibrium distribution, as is the resistance  $R_p$  (for which the plasma electron temperature and effective ion charge  $Z_{eff}$  must be assumed). The plasma, therefore, is not treated as a perfect conductor, but rather consumes flux resistively. The finite resistance of the plasma can be important over a DIII-D discharge of 5–6 s, with typical plasma resistive decay ( $L/R$ ) time of 20 to 50 s. The plasma current is represented by the current density on a computational grid corresponding to the nominal equilibrium derived by the EFIT magnetics fitting equilibrium reconstruction code [9]. The shape of the current density distribution is fixed at the nominal equilibrium while the total current ( $I_p$ ) is allowed to vary. Plasma current displacement is assumed to have only two degrees of freedom corresponding to rigid vertical and major radial motions of the equilibrium current density distribution.

The normalized co-prime factorization (NCF) design technique [10] was used to derive controllers from the linearized plant. In this method, input and output weighting matrices specify relative importance among the controlled parameters, applied voltages, and control coil current variations. For the experimental implementation, a single controller based on a plant linearized around a LSN ohmic (inductively heated) plasma equilibrium was used to control the entire discharge.

### 3.2. Plasma Control System Structure

Figure 2 shows an overview block diagram of the iso-flux plasma shape control using a MIMO controller. Magnetic diagnostic signals acquired by the PCS in realtime are used by the realtime EFIT algorithm to reconstruct the plasma equilibrium shape and current distribution, from which the X-point location and control point flux errors are calculated. These errors are processed by the MIMO shape

control algorithm to produce demand voltages for choppers on each shaping coil. A separate set of chopper voltage controllers is used to provide closed loop control of the choppers and thus produce the demanded voltages. The “standard” PID isoflux mode of shape control in DIII-D does not make use of separate chopper voltage control loops. This approach was taken to avoid having to include the highly nonlinear set of chopper models in the plant to be controlled. A fast, vertical stability control algorithm is also executed within the PCS. This controller does not actually stabilize the plasma, since it has no proportional feedback term. Instead it reduces the growth rate sufficiently that the slower shape control algorithm can stabilize the plasma.

This MIMO controller also operates on coil current “errors” in order to prevent coil limits from being encountered. Coil currents too near zero can cause choppers to latch (a type of fault), while currents exceeding maximum current limits will cause an overcurrent fault. In either case, the plasma discharge is ended. In order to avoid these failure modes, a coil current reference vector is constructed as a heavily filtered version of actual coil currents whenever currents are not near their limits. This reference is modified so as to produce large resultant error signals as currents approach a limit.

### 3.3. Controller Test Simulations

Testing of controller designs was performed using a detailed simulation of the system response, connected directly to the PCS implementation of the MIMO controller [11]. The simulator, shown schematically in Fig. 3, is built in the Matlab/Simulink™ environment and includes both linear plasma-conductor models and nonlinear power supply models. The PCS interfaces with the simulation in exactly the same way it interfaces with the actual tokamak systems, allowing realistic testing of both the controller itself and its implementation in the PCS. The simulation receives actuator commands from the PCS (point “A” in

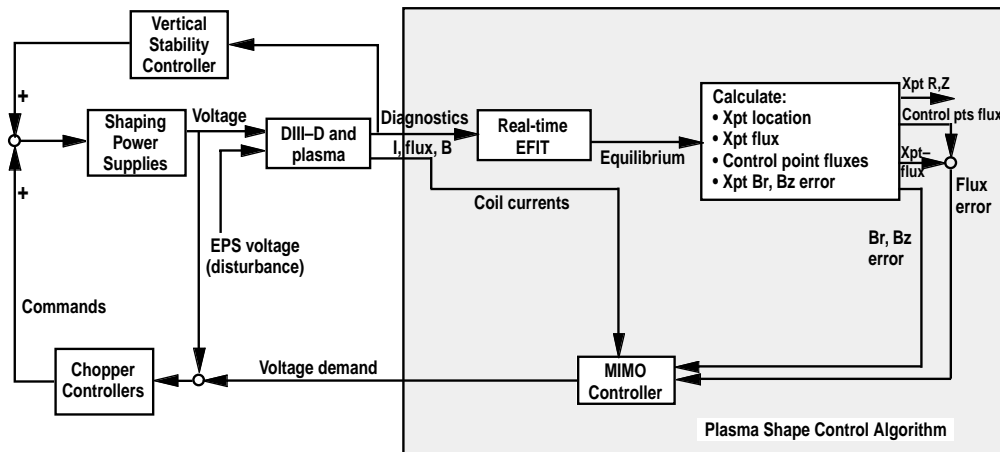


Fig. 2. Overview of MIMO isoflux control scheme.

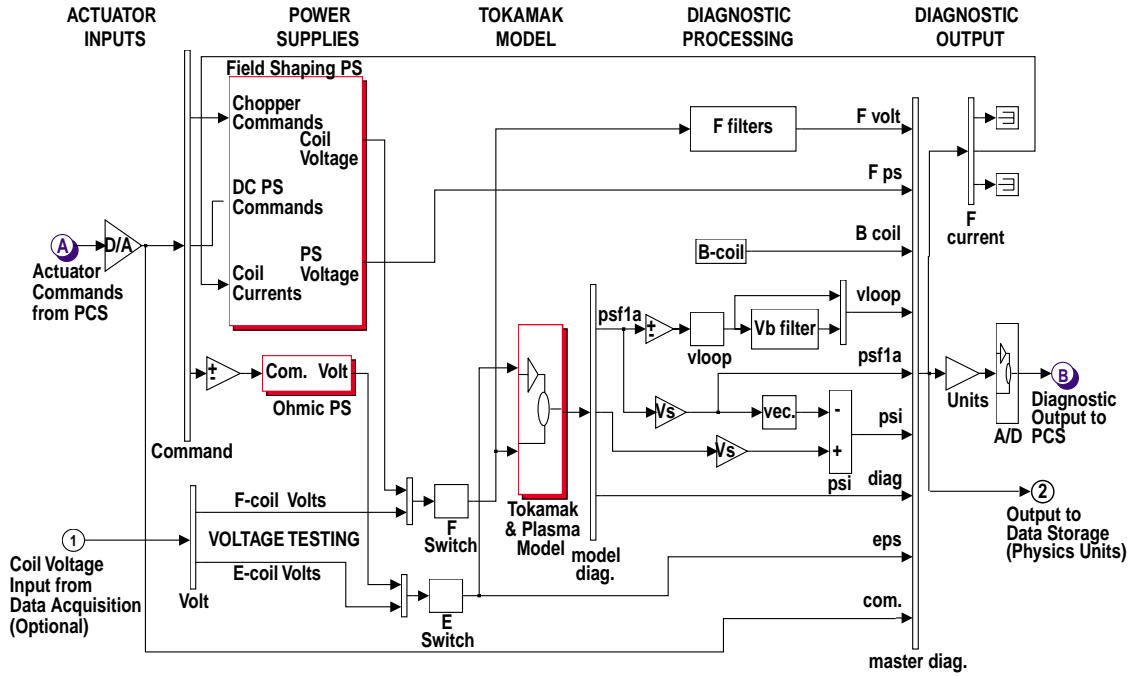


Fig. 3. Schematic of the detailed simulator used for testing of the PCS implementation of the controller without consumption of experimental machine time.

Fig. 3) and outputs magnetic diagnostic values corresponding to the simulated conductor current variation and plasma motion (point “B” in Fig. 3).

The detailed simulation allows testing of the PCS implementation, as well as iterative improvement of the controller itself, without the need for actual experimental machine time. This ability to test and optimize offline is a key benefit of model-based controller design, and is expected to save a significant amount of DIII-D experimental time presently devoted to empirical control tuning.

#### 4. IMPLEMENTATION OF MODEL-BASED MULTIVARIABLE CONTROLLER ON DIII-D

Figure 4 illustrates the requested (x) and actual (solid) plasma boundary during plasma discharge 99350, one of several discharges controlled by a model-based multivariable controller. This first implementation of a MIMO controller on DIII-D provided good steady state control, but quality of control during dynamic variation of plasma shape was mixed. Plasma control was always stable and was used to control several full shots from plasma current rampup through rampdown.

The MIMO control was first introduced in the middle of several ohmic discharges, then extended to the entire plasma current rampup and flatop phases for later discharges. Steady state plasma shape control was quite good in general, although accuracy of the upper isoflux control

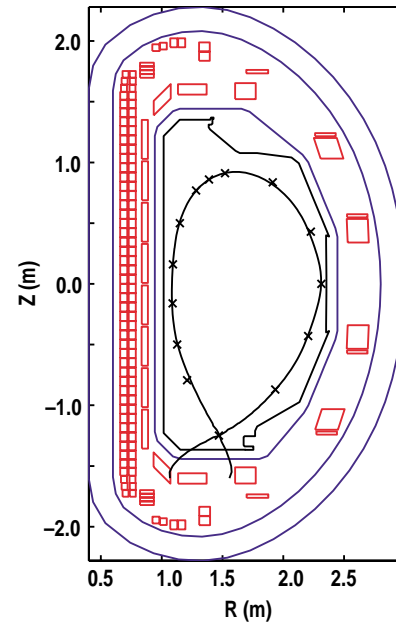


Fig. 4. DIII-D cross-section showing requested plasma boundary location (x) and actual (solid) boundary location controlled by MIMO controller in shot 99350 (time = 1490 ms).

points was somewhat worse than the lower control points and the X-point.

Figure 5 shows two shots in which the requested plasma shape changed with time. Control of the X-point was

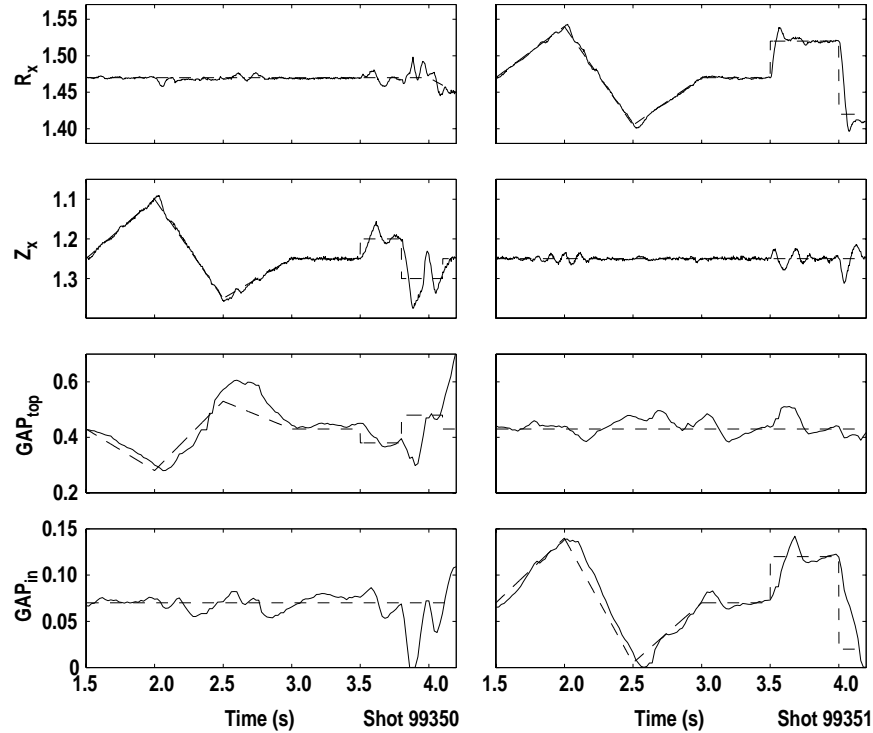


Fig. 5. Example of control in two shots with requested plasma shape changing over time (all units in meters). Solid lines indicate achieved values, while dashed lines denote target values.

still generally very good in this case, but flux at the upper control points followed their requests relatively slowly. In shot 99350, an approximately rigid vertical motion of the plasma was programmed between 1.5 s and 4.2 s. In shot 99351, an approximately rigid radial plasma motion was programmed in the same interval. The programmed radial motion was generally better behaved than the vertical motion, even during the sudden steps starting at 3.5 s. The large ringing on the X-point vertical position ( $Z_x$ ) following the requested step change also couples to the radial control to produce poor control of the inside gap ( $GAP_{in}$ ). This problem was found to be due to inaccuracies in the model of the closed-loop vertical stability control used in the control design (see Fig. 2). These inaccuracies have been corrected since this implementation, and closed-loop simulations using the corrected vertical stability control model reproduce the behavior observed in the experiment.

Performance of the MIMO controller is also somewhat affected by plasma internal inductance ( $l_i$ ) – a measure of the “peakedness” of the current distribution within the plasma. The internal inductance naturally increases throughout an ohmic discharge as the profile evolves toward its steady state condition. Figure 6 illustrates X-point position control and control of the top plasma-wall gap during 300 ms intervals at low  $l_i$  ( $\sim 1.0$ ) and high  $l_i$  ( $\sim 1.25$ ) in discharge 99350. The standard deviation of X-point control errors decreases with increasing  $l_i$  experiencing a dramatic reduction in the amplitude of a low frequency ( $\sim 10$ – $11$  Hz) oscillation prominently observed at low  $l_i$ . The mean value of the

X-point vertical ( $Z_x$ ) and radial ( $R_x$ ) position appears to be unaffected by the  $l_i$  value. The general variation in X-point control with  $l_i$  is likely the result of controller optimization for a relatively high  $l_i$  equilibrium, corresponding to the plasma state in the interval  $3.2 < t < 3.5$  s in discharge 99350. The value of  $l_i$  strongly affects vertical growth rate and response, which in turn strongly affects the controller design and response.

In contrast with the improvement in X-point control with increasing  $l_i$ , accuracy of top gap control is clearly reduced as  $l_i$  increases. Comparison of the two lowest frames in Fig. 6 shows a mean achieved gap distance (solid line) of  $\sim 0.5$  cm from the target value (dashed line) in the lower  $l_i$  case, while the mean error in gap distance exceeds 1.5 cm in the higher  $l_i$  case. Since increasing  $l_i$  corresponds to a peaking of the current profile and resulting increase in effective distance of the current channel from control coils, increased coil current is necessary to regulate the plasma surface as  $l_i$  increases. The heavy weighting of X-point control relative to upper gap control inherent in the design of this controller produced a demand of insufficient current in the upper coils to accurately regulate this particular region of the separatrix in the higher  $l_i$  regime. Higher order moments of the current profile may influence this process as well, but are entirely ignored by the modeling process, controller design, and control operation.

Figure 7 illustrates modification of the shaping coil (F-coil: see Fig. 1) current reference signal in order to

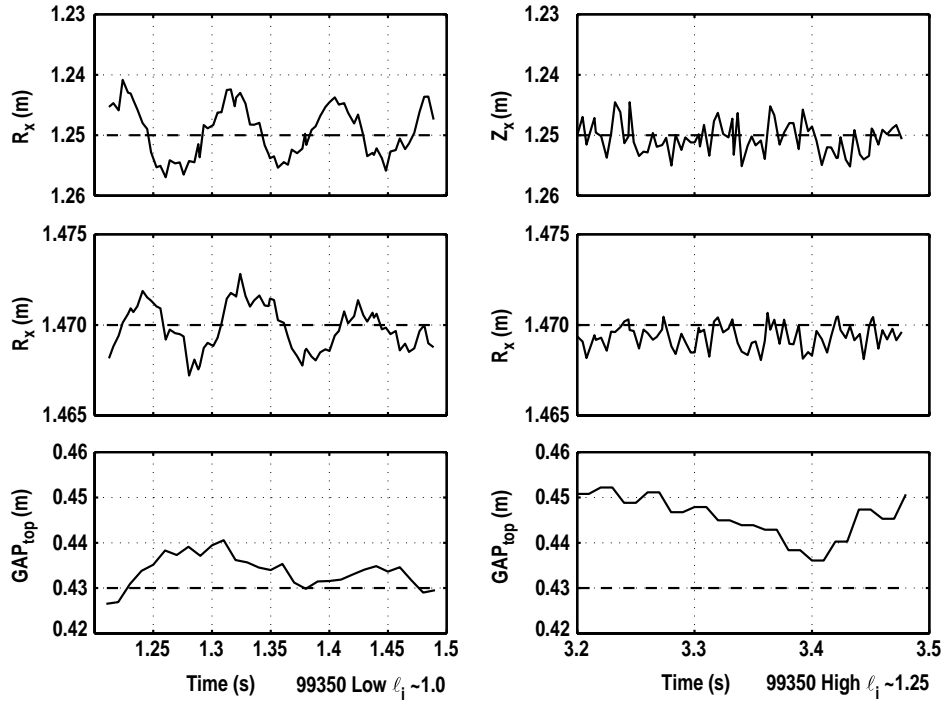


Fig. 6. Accuracy of X-point position control improves and accuracy of top gap control degrades with increasing internal inductance (discharge 99350). Solid lines indicate achieved values, while dashed lines denote target values.

avoid coil current limits from ending the shot. The reference signal is initialized to the value of the F-coil current when the MIMO controller takes over. It is subsequently computed as a heavily filtered version of the F-coil current except in the case where the current approaches either 0 or a maximum current limit. In these cases, the reference is

modified so as to induce the controller to “pull” the coil current away from the limit value. In Fig. 7(a) and (b), when the coil current value becomes less than 400 A, the current reference signal begins to grow larger. Figure 7(a) illustrates a case when competing control demands keep the

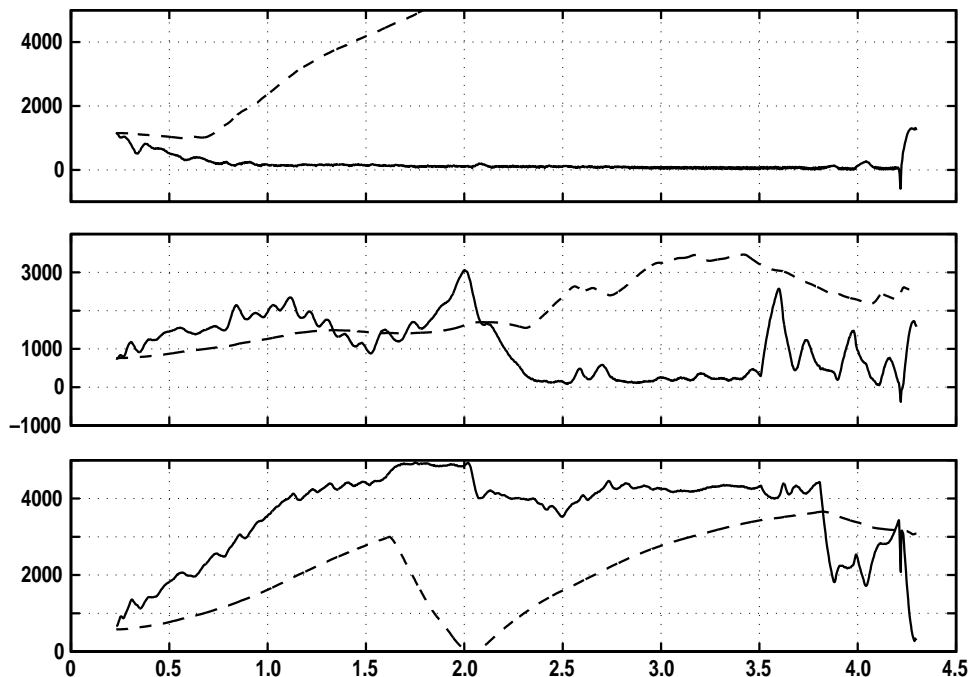


Fig. 7. F-coil current data (solid) versus reference signal (dashed) in shot 99350 for F-coils (a) F4B, (b) F5B, and (c) F8B.

current in coil F4A low despite the current reference modification. When the current increases to more than 400 A in Fig. 7(b), the reference signal tends back toward the measured coil current value. In Fig. 7(c), when the current comes close to the maximum limit of 5 kA, the reference signal moves down to maintain the current in the F8B coil below the limit. Changes in coil current between 1.5 and 4 s seen in the plots of the F5B and F8B coils correspond to the programmed plasma shape perturbations shown in Fig. 5.

## 5. SUMMARY

A model-based multivariable controller has been successfully implemented and tested experimentally on the DIII-D tokamak. Steady state control was quite good in general, with accuracy of control of upper portions of the plasma somewhat worse than lower portions and the X-point. Quality of control in tracking of changing plasma shape requests was mixed, with X-point control remaining very good while some upper plasma-to-wall gaps in some shots were not very well controlled. The higher accuracy of the X-point was consistent with much higher weighting given to its regulation in the NCF design process. The MIMO controller successfully controlled the plasma throughout all phases of the discharge, including plasma current rampup, flattop, and rampdown. The controller always provided stable control despite the wide range in  $I_i$  always experienced over these periods and the relatively high  $I_i$  of the design point on which the controller was based. Some of the control inaccuracies which occurred were not unexpected, since there were known inadequacies in accuracy of some models, especially that of the closed-loop vertical control. The significant dependence of control accuracy on the value of  $I_i$  (and perhaps higher order moments of the current profile) in particular may indicate a need for gain-scheduling.

Additional development is needed before MIMO controllers can be routinely used during DIII-D experimental operations, although solutions to some practical operational concerns, including coil current limiting, were demonstrated in the initial implementation. Other practical issues which must be addressed include: antiwindup for chopper voltage saturations, gain scheduling of multiple controllers (with associated techniques for achieving bumpless transfer), limiting a particular buss voltage, resolving conflicts between fast vertical and slow shaping control, and dealing with multiple unsynchronized processors with varying cycle times in the PCS.

In the long term, it is expected that DIII-D MIMO controllers will integrate shape control with control of pressure, radial E-field, and current profiles using feedback commands to new actuators such as counter-injection neutral beams, electron cyclotron heating, and electron cyclotron current drive.

## ACKNOWLEDGEMENTS

This work was supported by the U.S. Department of Energy under Contract No. DE-AC03-99ER54463.

## References

- [1] ARIOLA, M. AMBROSINO, G., LISTER, J.B., PIRONTI, A., VILLONE, F., VYAS, P., "A Modern Plasma Controller Tested on the TCV Tokamak," *Fusion Technology* **36** (1999) 126.
- [2] VILLONE, F., VYAS, P., LISTER, J.B., ALBANESE, R., "Comparison of the CREATE-L Plasma Response Model with TCV Limited Discharges," *Nucl. Fusion* **37** (1997) 1395.
- [3] HUMPHREYS, D.A., WALKER, M.L., "Minimal Plasma Response Models for Design of High Betap Tokamak Shape and Position Controllers," General Atomics Report GA-A23321 (to be printed); submitted for publication in *Fusion Technology* (April 2000).
- [4] FERRON, J.R., WALKER, M.L., LAO, L.L., ST.JOHN, H.E., HUMPHREYS, D.A., LEUER, J.A., "Realtime Equilibrium Reconstruction for Tokamak Discharge Control," *Nucl. Fusion* **38** (1998) 1055.
- [5] KINOSHITA, S., *et al.*, "Independent control of gaps in single-null divertor discharges on the DIII-D tokamak," General Atomics Report GA-A19584 (1989).
- [6] WALKER, M.L., NEREM, A., BAGGEST, D., "Advanced Plasma Control IR&D Final Report, Part I: DIII-D System Models for Feedback Control," General Atomics Report GA-C21745 (1996).
- [7] ALBANESE, R., COCCORESE, E., RUBINACCI, G., "Plasma Modeling for Vertical Instabilities," *Nucl. Fusion* **29** (1989) 1013.
- [8] HUMPHREYS, D.A., HUTCHINSON, I.H., "Axisymmetric Magnetic Control Design in Tokamaks Using Perturbed Equilibrium Plasma Response Modeling," *Fusion Technology* **23** (1993) 167.
- [9] LAO, L.L., ST.JOHN, H., STAMBAUGH, R.D., KELLMAN, A.G., PFEIFFER, W., "Reconstruction of Current Profile Parameters and Plasma Shapes in Tokamaks," *Nucl. Fusion* **25** (1985) 1611.
- [10] McFARLANE, D.C., GLOVER, K., "Robust controller design using normalized coprime factor plant descriptions," Springer-Verlag, *Lect. Notes in Control and Inf. Sci.* **138** (1989).
- [11] LEUER, J.A., WALKER, M.L., HUMPHREYS, D.A., FERRON, J.R., NEREM, A., PENAFLO, B.G., "Development of a Closed Loop Simulator for Poloidal Field Control in DIII-D," *Proc. 18th IEEE/NPSS Symp. on Fusion Engineering*, October 25-29, 1999, Albuquerque, New Mexico, to be published; General Atomics Report GA-A23266 (1999).